



Review of 3D templates for in silico homology models of MATs: improved 3D model of hDAT

Charles B. Jones¹ · Małgorzata Dukat¹

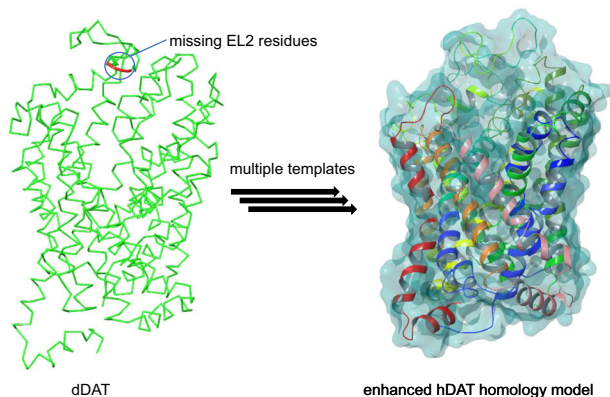
Received: 9 June 2021 / Accepted: 12 February 2022 / Published online: 3 March 2022

© The Author(s), under exclusive licence to Springer Science+Business Media, LLC, part of Springer Nature 2022

Abstract

In the past 20 years there have been great leaps in the understanding of the structure and mechanism of monoamine transporters (MATs) owing to X-ray crystallography and cryo-EM. From the first breakthrough with the crystallization of the ortholog bacterial leucine transporter (LeuT) to more recent structures of the higher-identity drosophila dopamine transporter (dDAT) and human serotonin transporter (hSERT), the construction of better 3D computational models of hDAT has been pursued and is essential for the development of new medications for neuropsychiatric disorders associated with dopamine dysregulation. Previous and recent homology models of the yet to be crystallized hDAT have relied only on one template for generation. Here, we tabulated currently available crystal structures of MATs and then employed a multi template approach to generate a hDAT 3D homology model where contribution of individual templates account for missing structural features of single template models (i.e., EL2 in dDAT).

Graphical abstract



Keywords Monoamine transporters · Human dopamine transporter · NET · SERT · X-ray structures · 3D homology modeling

Supplementary information The online version contains supplementary material available at <https://doi.org/10.1007/s00044-022-02863-5>.

✉ Małgorzata Dukat
mdukat@vcu.edu

¹ Department of Medicinal Chemistry, School of Pharmacy, Virginia Commonwealth University, Richmond, VA 23298, USA

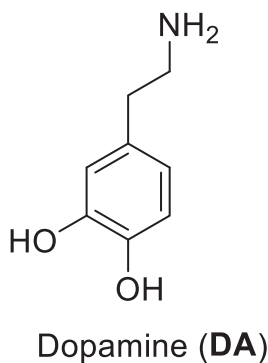
Introduction

The dopamine transporter (DAT), one of the three high-affinity, low-capacity monoamine transporters (MATs), belongs to the solute carrier 6 (SLC6) family, the largest group of membrane transporters, and plays an important role in homeostasis of a healthy neuron [1]. The other two MATs are the serotonin transporter (SERT; SLC6A4) and the norepinephrine transporter (NET; SLC6A2). On the basis of the primary amino acid sequence similarity (~40%)



Fig. 1 Alignment of LeuT, hSERT, dDAT, hDAT, and hNET. Symbols represent: (*) identity, (:) high similarity, (-) similar, and blank space is non similar

(Fig. 1) and mutagenesis studies it was assumed that all three MATs are structurally similar. Particularly, DAT (SLC6A3) guards the synaptic concentration of the endogenous amine neurotransmitter dopamine (DA) and is implicated in a multitude of neuropsychiatric disorders. In addition, DAT transports a variety of xenobiotics. Thus, it is critical to understand the interaction of human DAT (hDAT) with a substrate/inhibitor on a molecular level to guide structure–activity relationship studies when developing new pharmacological tools and/or pharmaceutical entities.

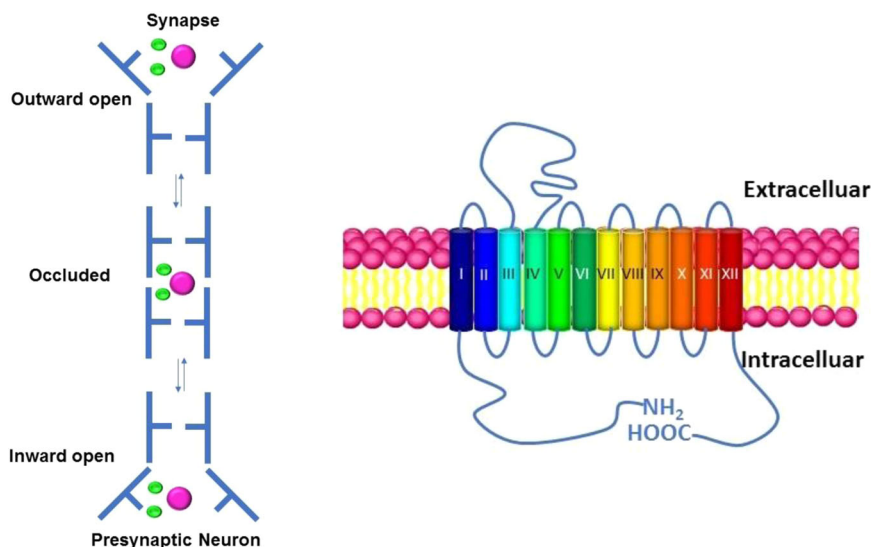


The functional mechanisms and crystal structures of some MATs have been elucidated in the past two decades. Despite the advancements in structural biology, a hDAT crystal structure is still lacking. Nevertheless, homology modeling can be used as a surrogate approach to explore hDAT. Using the most recent homologs with high identity compared to hDAT it is possible to develop a more accurate model than has been used in the past. With new crystal structures being solved that are closer to hDATs' identity and total peptide chain length, new and improved homology models can be generated to study the inner workings of hDAT through docking and molecular dynamics. In this paper we briefly review a history of MAT crystal structures followed by recommendations on improved hDAT homology model generation based on our *in silico* studies.

Agents

Besides the endogenous neurotransmitters that interact with MATs during normal function two other types of agents act directly with MATs. The first type of agent are reuptake inhibitors (blockers). These agents bind in the central binding site (S1) of the outward facing conformation and prevent the MAT from going through the transport cycle.

Fig. 2 Left panel: Schematic representation of the translocation mechanism of substrate (magenta) and Na^+ ions (green) in MATs (i.e., DAT). Right panel: A 2D representation of a monoamine transporter depicting 12 transmembrane-spanning helices connected via intra- and extracellular loops with intracellular amine and carboxyl termini



Blockers binding also prevents endogenous neurotransmitters from interacting with MATs. There are known MAT-selective and nonselective blockers. For example, selective blockers include agents that are used to treat depression such as the selective serotonin reuptake inhibitor fluoxetine (Prozac). Cocaine, one of the better-known drugs of abuse, is a nonselective blocker at all three MATs [1]. The other type of agents that interact with MATs are releasing agents (substrates) [1]. These agents bind at the S1 site of the outward facing conformation and go through the transport cycle to be released intracellularly but cause the MAT to transition into a reverse cycle which transfers intracellular neurotransmitter extracellularly [1]. Methamphetamine, a well-known drug of abuse, is a nonselective substrate for MATs. Both blockers and substrates have the same overall outcome of increasing extracellular neurotransmitter concentration [1].

Transport cycle

MATs assume three different conformations through neurotransmitter translocation (Fig. 2). The conformations are known as outward-open facing, occluded, and inward-open facing [1]. The mechanism by which the MATs transition through the three states is known as the *alternating access model* [1]. Along with transport of the neurotransmitters, the MATs also cotransport ions. SERT cotransports one 5-HT with one Na^+ and one Cl^- ion together with the counter transport of one K^+ ion. Whereas both NET and DAT cotransport NE and DA, respectively with two Na^+ ions and one Cl^- ion [1]. The alternating access model mechanism is initiated when the MAT is in the outward-open facing conformation and the cotransported ions bind on the extracellular side. This is followed by a substrate binding at the S1 site from the extracellular side which prompts the

MAT to transition into a closed occluded state. In the occluded state the substrate and ions are blocked from both the extracellular and intracellular surfaces. The MAT then transitions into the inward-open facing state which releases the substrate and ions via diffusion. Once the MAT is emptied in the inward-open facing conformation it transitions empty back through the occluded state and then to the outward-open facing conformation to renew the cycle. For SERT, this final progression counter transports one K^+ ion.

Leucine transporter (LeuT)

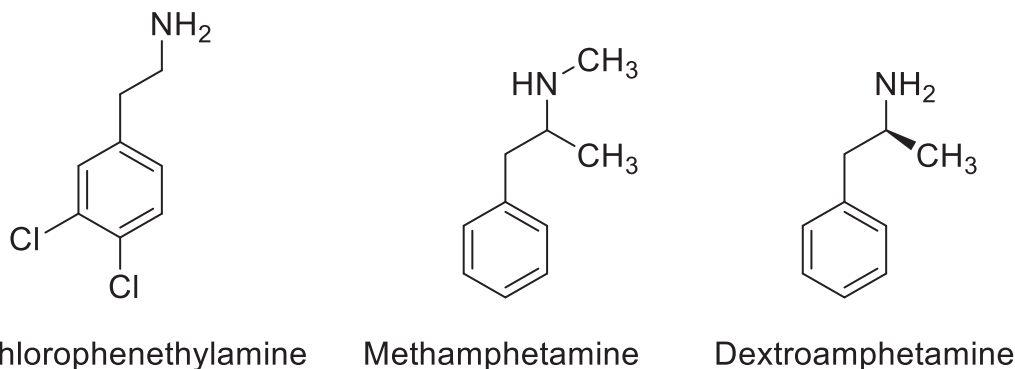
The first homolog of a monoamine transporter to be crystallized was the leucine transporter (LeuT) from the bacterium *Aquifex aeolicus* [2]. This was a breakthrough in elucidations of the tertiary structure and function of transporters and granted 3D molecular modeling studies. LeuT was crystallized in 2005 [2] and was shown to consist of 12 transmembrane-spanning helices with a pseudo-2-fold axis in the membrane plane, connected via intra- and extracellular loops with both amino and carboxyl termini located intracellularly (Fig. 2). The protein shares 20% identity with the eukaryotic Neurotransmitter-Sodium Symporters i.e., MATs [2]. There are currently 22 published crystal structures of LeuT with multiple drugs that are in various states of the transport cycle.

Drosophila melanogaster dopamine transporter (dDAT)

The first of the MATs to be crystallized in 2013, was from the fruit fly *Drosophila melanogaster* (i.e., dDAT) [3]. The dDAT crystal structure was a leap forward in modeling the human dopamine transporter (hDAT) as it shares greater than 50% identity [3]. Several mutations and modifications were

Table 1 Summary of current dDAT crystal structures [3–5]

PDB ID ^a	Resolution (Å) ^b	Agents	Mutation	Author, ref.
Inhibitors				
4M48	2.96	Nortriptyline	V74A/V275A/V311A/G538L/L415A	Panmatsa et al. [3]
4XP5	3.3	RTI55	V74A/L415A	Wang et al. [4]
4XPG	3.21	WIN35428	D121G/S426M	Wang et al. [4]
4XPB	3.05	Cocaine	D121G/S426M	Wang et al. [4]
4XPF	3.27	RTI55	D121G/S426M	Wang et al. [4]
4XP4	2.8	Cocaine	V74A/L415A	Wang et al. [4]
4XNU	2.98	Nisoxetine	V74A/V275A/V311A/G538L/L415A	Penmatsa et al. [5]
4XNX	3	Reboxetine	V74A/L415A	Penmatsa et al. [5]
Releasers				
4XPH	2.9	3,4-Dichlorophenethylamine	D121G/S426M	Wang et al. [4]
4XP6	3.1	Methamphetamine	V74A/L415A	Wang et al. [4]
4XPT	3.36	3,4-Dichlorophenethylamine	D121G/S426M	Wang et al. [4]
4XPA	2.95	3,4-Dichlorophenethylamine	V74A/L415A	Wang et al. [4]
4XP9	2.8	Dextroamphetamine	V74A/L415A	Wang et al. [4]
Endogenous				
4XP1	2.89	Dopamine	V74A/L415A	Wang et al. [4]

^aProtein Data Bank ID^bX-ray method**Fig. 3** Structures of the DAT releasing agents co-crystallized with dDAT in the S1 binding site

used to induce the transporter to crystallize. Point mutations V74A, V275A, V311A, L415A, and G538L were used [3]. Amino acid residues 1–20 as well as extracellular loop 2 (EL2) 164–206 were removed [3]. Amino acids 602–607 were replaced by a C-terminus green fluorescent protein (GFP–His8) tag with a thrombin cleavage site (LVPRGS) [3]. Recombinant Human Anti-Dopamine transporter antibody antigen binding fragment (Fab) 9D5 at a ratio of DAT:Fab 1:1.1 was also used to enhance crystallization [3]. There are 14 current crystal structures of dDAT bound to either releasing agents or reuptake inhibitors (Table 1).

All structures are either in the outward facing state (from inhibitors) or in the partially occluded state (from releasing agents). The inward facing and occluded conformations

have still not been reported. The releasing agents crystallized with dDAT are 3,4-dichlorophenethylamine, methamphetamine, and dextroamphetamine (Fig. 3) [4]. The uptake inhibitors that have been co-crystallized are nisoxetine, reboxetine, RTI55, WIN 35,428, cocaine, and nortriptyline (Fig. 4) [3–5]. DA, the endogenous ligand, has also been crystallized with dDAT [4].

Human serotonin transporter (hSERT)

The hSERT was first crystallized in 2016 [6]. There are currently three different constructs of the crystallized transporter: the N- and C-terminally truncated wild type (Δ N72, Δ C13), ts3 which contains the thermostabilizing mutations

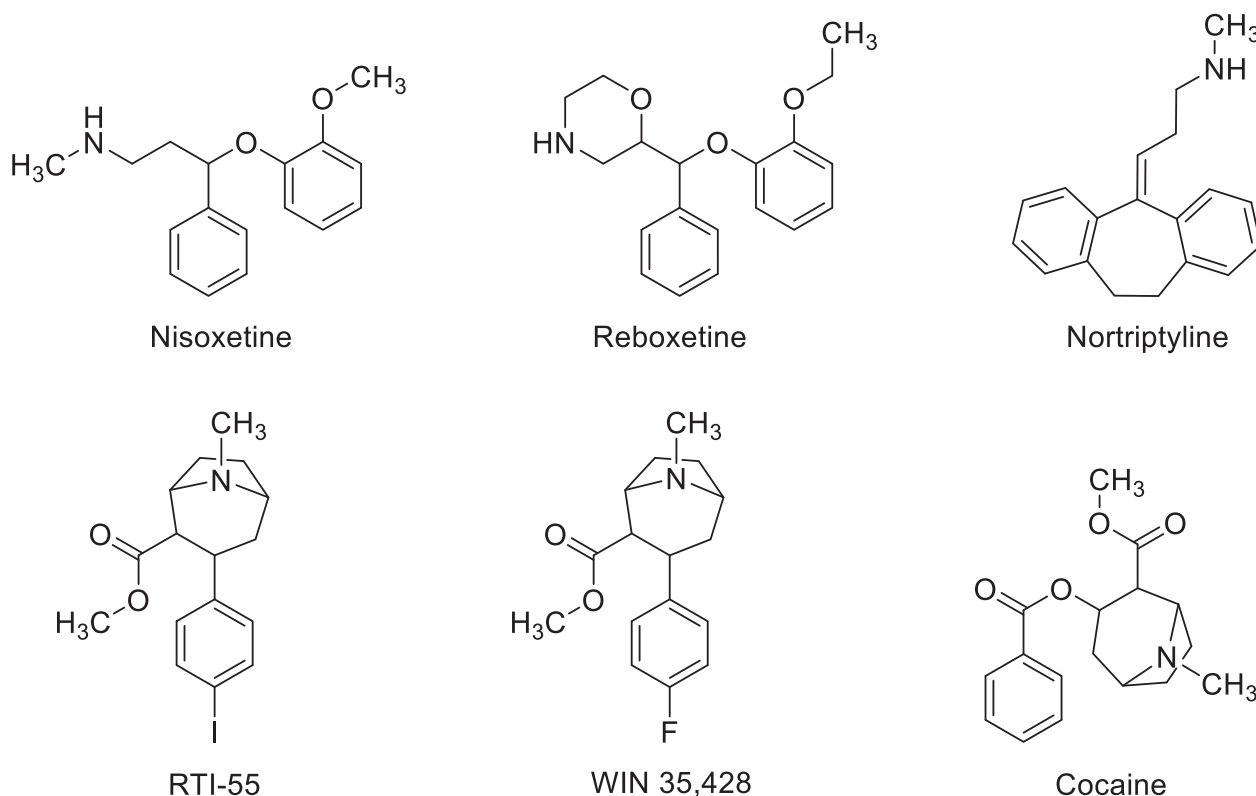


Fig. 4 Structures of the DAT uptake inhibitors co-crystallized with dDAT in the S1 binding site

Y110A, I291A, and T439S, and ts2 which is identical to ts3 without the Y110A mutation [6]. ts2 and ts3 also have had mutations of the surface-exposed cysteines C554A, C580A, and C622A [6]. These constructs are then fused to a C-terminus green fluorescent protein (GFP) and then tagged with twin Strep and a decahistidine for purification [6]. Two different recombinant antibody fragments have also been used to help crystallization, Fab 8B6 and 15B8 [6]. Only Apo-state hSERT and reuptake inhibitors bound in hSERT have been crystallized. These inhibitors are Br-citalopram, (*S*)-citalopram (escitalopram), paroxetine, sertraline, fluvoxamine, Br-paroxetine, and levoparoxetine [6–9].

Not only are there X-ray crystal structures but also cryo-EM structures for hSERT are reported. Thanks to cryo-EM and identification of the non-competitive inhibitor ibogaine, all conformations (outward facing, partially occluded, occluded, and inward facing) of hSERT have been detailed [7]. Also, using citalopram, orthosteric and allosteric sites of hSERT have been identified [6]. There are currently 19 published structures of hSERT (Table 2).

Lacking crystal structures

The third MAT, the NET, has yet to be crystallized. Other unreported crystal structures are SERT with releasing agents, hDAT, DAT with its occupied allosteric site, DAT

occluded, DAT inward facing, and any of the above transporters with a partial releaser.

Literature homology modeling

The first hDAT homology model generated using the LeuT crystal structure as a template was reported in 2007 [10]. While LeuT has a low % identity and query coverage (the % of the contiguous length that aligns with the NCBI hit) compared to hDAT, all three conformations of the transport cycle were crystallized. After the crystal structure of dDAT was elucidated in 2013, it was used as the next step forward in hDAT 3D homology modeling studies [3, 11]. Thus, an actual DAT crystal structure was available to generate hDAT homology models. The first report of an hDAT homology model generated using dDAT crystal structure (PDB ID: 4M48) as a template was reported in 2015 [11]. Also, in this same year a burst of dDAT crystal structures that make up the remainder of the currently reported dDAT crystal structures were elucidated [4, 5]. The following year a human MAT i.e., hSERT was for the first time crystallized and the structure reported [6]. hSERT no longer needed homology model development due to the presence of the newly solved crystal structures. However, it seemed that most homology models of hDAT were still being developed only from the dDAT template [12]. Several homology models had been published using either dDAT PDB

Table 2 List of currently available hSERT crystal structures [6–9]

PDB ID	Method	Resolution (Å)	Agents	Mutation	Author, ref.
5I6Z	X-ray	4.53	Apo	ts2	Coleman et al. [6]
5I74	X-ray	3.395	Br-Citalopram	ts3	Coleman et al. [6]
5I73	X-ray	3.24	Escitalopram	ts3	Coleman et al. [6]
5I75	X-ray	3.49	Escitalopram, Br-Citalopram	ts3	Coleman et al. [6]
5I6X	X-ray	3.14	Paroxetine	ts3	Coleman et al. [6]
5I71	X-ray	3.15	Escitalopram	ts3	Coleman et al. [6]
6AWO	X-ray	3.534	Sertraline	ts3	Coleman et al. [9]
6AWN	X-ray	3.62	Paroxetine	S439T	Coleman et al. [9]
6AWQ	X-ray	4.046	Sertraline	ts3	Coleman et al. [9]
6AWP	X-ray	3.8	Fluvoxamine	ts3	Coleman et al. [9]
6W2B	X-ray	4.7	Br-Paroxetine	ts2	Coleman et al. [8]
6W2C	X-ray	6.3	Levoparoxetine	ts2	Coleman et al. [8]
6DZW	Cryo-EM	4.3	Paroxetine	ts2	Coleman et al. [7]
6DZV	Cryo-EM	4.2	Ibogaine	WT	Coleman et al. [7]
6DZY	Cryo-EM	4.1	Ibogaine	ts2	Coleman et al. [7]
6DZZ	Cryo-EM	3.6	Ibogaine	WT	Coleman et al. [7]
6VRK	Cryo-EM	4.1	Br-Paroxetine	WT	Coleman et al. [8]
6VRL	Cryo-EM	3.8	Levoparoxetine	WT	Coleman et al. [8]
6VRH	Cryo-EM	3.3	Paroxetine	WT	Coleman et al. [8]

Table 3 Comparison of crystal structure templates % identity and query coverage compared to hDAT used for current and previously generated homology models [10–12]

Transporter	Template PDB ID	% Identity	Query coverage ^a	Author, ref.
LeuT	2A65_A	24.95	77%	Huang and Zhan [10]
dDAT	4M48_A	54.81	88%	Yuan et al. [11] Haddad et al. [12]
dDAT	4XPA_A	54.63	88%	Haddad et al. [12]
dDAT	4XPB_A	55.35	88%	Employed in current study
dDAT	4XPT_A	55.33	87%	Employed in current study
hSERT	6VRH_A	50.00	92%	Employed in current study

^aThe % of the contig length that aligns with the NCBI hit. A small query coverage % means only a tiny portion of the contig is aligning. If there is an alignment with 100% identity and a 5% query coverage, the sequence is probably not that taxon

ID: 4M48 or 4XPA (Table 3). Currently there is only one hDAT homology model reported using hSERT as a template [13]. This hDAT model by Ortore et al. [13] was developed exclusively for docking inhibitors. The model was generated using only two crystal structure-bound inhibitors (dDAT PDB:4XP4 and hSERT PDB: 5I6X) as templates and simulated annealing and no template was used to generate EL2.

Results and discussion

An improved 3D homology DAT model

Steps we employed in generating, evaluating, and validating the generation of a new hDAT homology model that can be used for docking and molecular dynamics are as follows:

Step 1

Obtain hDAT target sequence from NCBI GenPept protein database.

Accession code BAA22511.1.

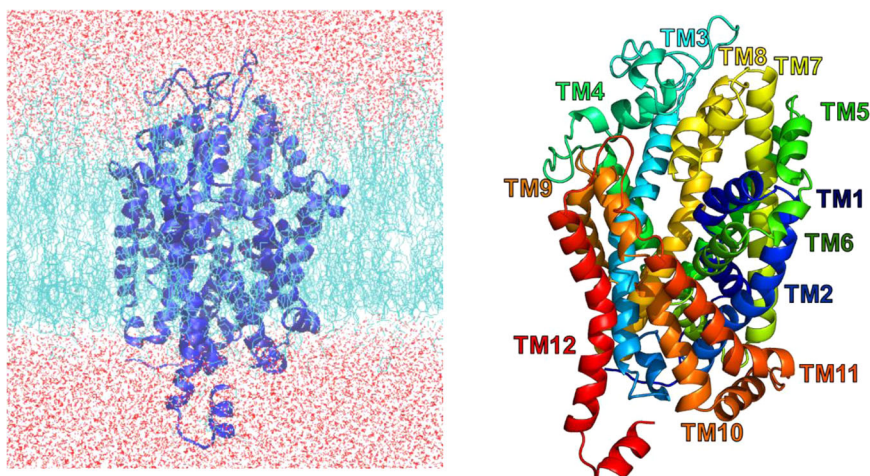
Step 2

Run BLAST on target sequence through PDB database to acquire sequences with significant alignments to hDAT (i.e., dDAT, hSERT) [14].

Step 3

Obtain best fitting dDAT and hSERT crystal structure templates from NCBI GenPept [4, 8].

Fig. 5 Left panel: Molecular dynamics simulation of hDAT homology model (new cartoon, blue) embedded in a lipid bilayer (lines, cyan) and surrounded by water box (lines, red) generated from CHARMM and displayed in VMD. Right panel: hDAT homology model (cartoon) with transmembrane (TM) helices labeled and colored



PDB IDs: 4XPB_A, 4XPT_A, and 6VRH_A (Table 3).

Step 4

Use most recent version of MODELLER to run alignments and generate 100 models based on multi template setup [15].

Step 5

Evaluate best model from scoring functions (i.e., DOPE, GA341) [15, 16].

Step 6

Truncate any portions of the model not properly generated (i.e., residues 1–54).

Step 7

Analyze conformational properties of the model using PROCHECK to generate Ramachandran plot (shown in Online Resource 1, Fig. S1) and ProTable.

Step 8

Use CHARMM [17] to generate lipid bilayer and water box for molecular dynamics studies (Fig. 5) and as shown in the animation (Online Resource 2).

Step 9

Validate model (Fig. 5) by docking previously crystallized ligand and compare RMSD (i.e., dock cocaine and 3,4-dichlorophenethylamine using GOLD 2020 [18]; docking images Figs. S2, S3 are given in Online Resource 1).

While LeuT is a homolog of MATs and was essential in the understanding of the conformation changes that take place in the alternating access model, it is overall a poor choice for hDAT homology model generation today because there are many more closely related proteins with much higher % identities to hDAT than LeuT. Currently, dDAT is the most accurate single template available for hDAT homology modeling. dDAT only has outward-open facing crystal structures and therefore hDAT homology models of occluded and inward-open facing cannot be generated using dDAT as a template alone. Another issue that has plagued hDAT homology model development is that the EL2 is not able to be properly modeled from dDAT due to its removal for the crystal structures that have been reported. This is often not an issue if only binding studies of the S1 site are to be performed. If MD simulations were to be attempted, on the other hand, this might become an issue. To amend this issue the crystal structure of hSERT, that possesses an intact EL2, might be used to model this portion of the hDAT homology model. Generation of a hDAT homology model using only the hSERT crystal structure as a template is not recommended as the dDAT crystal structures have a higher % identity and use the same endogenous ligand as hDAT. Furthermore, our molecular dynamics studies displayed resulted in a stable protein embedded in the lipid bilayer under the time constraints employed. Thus, our model might be used to not only investigate the binding modes of ligands in the S1 site but also to explore extra-cellular interactions involving the ELs or simulations where entire protein conformational changes are of interest.

To validate our model we docked both cocaine (a blocker) and 3,4-dichlorophenethylamine (a releasing agent) and compared the docking solutions with the binding mode of cocaine and 3,4-dichlorophenethylamine in the co-crystal structure (PDB ID: 4XPB and 4XPT, respectively) and found that the new model retained/mimicked the

structural features necessary for binding both blocker and releasing agent (Figs. S2, S3, respectively; Online Resource 1). Both test ligands resulted in solutions that matched the pose and retained an essential salt bridge interaction with the N atom of the ligands and carboxylate anion D79 of hDAT in the corresponding dDAT (D46) crystal structures, validating the hDAT homology model.

Since the two main types of agents that interact with DAT are blockers and releasing agents, using crystal structure-blocker and -releasing agent complexes as templates (i.e., PDB ID: 4XPB and 4XPT, respectively) might benefit docking studies by generating a “dual-purpose” homology model. This might be attributed to specific molecular interactions between the protein/ligand complex that account for a particular type of ligand. Furthermore, such a dual-purpose homology model might be employed in studies where the functional activity of chemical entities is unknown and should allow for docking both types of agents prior to determining their function.

Conclusions

We believe that using multiple crystal structures of homologous proteins will deliver a more realistic 3D homology model of the proteins of interest compared to use of a single crystal structure as a template. Here we demonstrated that using hSERT and two dDAT crystal structures together to generate hDAT homology models yielded a model that accounts for all extra and intracellular loops lacking in previous 3D models. With templates using a substrate as well as a blocker, docking can be conducted using both types of agents with specific molecular protein/ligand interactions being preserved. With the use of MODELLER, dDAT and hSERT crystal structures can be used in conjunction as templates for a hDAT homology model. Furthermore, molecular dynamics and binding studies can be employed to more accurately portray hDAT inner workings.

Methods

Homology models

One hundred homology models of hDAT were generated using MODELLER 9.24 and three crystal structures as a template [15]. The two highest identity dDAT crystal structures (PDB ID: 4XPB and 4XPT) at 55.35% identity as well as the greatest query coverage hSERT crystal structure (PDB ID: 6VRH) at 92% coverage were used [4, 8]. The original alignment of the structures was conducted using BLAST [14]. The sequences of dDAT, hSERT, and hDAT were obtained from genpept (accession codes 4XPB_A,

6VRH_A, and BAA22511, respectively). Due to the lack of corresponding residues, the first 54 residues from the N-terminus were not modeled. The homology model with the lowest discrete optimized protein energy (DOPE) score and highest GA341 score was then selected for further analysis and validation [15, 16]. GA341 is a multivariate scoring function that depends on compactness and combined statistical potential z-score of the model as well as the percentage sequence identity of the target-template alignment that was used to build the model [15, 16]. Candidate model was subjected to analysis through a PROCHECK, and ProTable, and then validated by the docking.

Protein analysis

PROCHECK and ProTable were used to analyze the lead hDAT homology model. PROCHECK examines the stereochemical quality of the hDAT structure, producing a number of plots analyzing its overall and residue-by-residue geometry. The Ramachandran plot (Fig. S1) generated by PROCHECK has 94.6% of the residues from the hDAT homology model in the most favored regions. A good quality model is expected to have over 90% of the amino acid residues in the most favored regions. ProTable uses a spreadsheet comparison and analysis of the hDAT homology model using well founded criteria. No bond lengths, omega torsion angles, or chiral atoms deviated from ideal. Only several residues had poor bond angles but were close to the 10 Å cutoff and none of these amino acid residues were within the S1 central binding pocket. The BioPolymer suite of SybylX 2.1.1 was used to compare the RMSD of the hDAT homology model and the dDAT template. The RMSD between all atoms of the two proteins was 2.16 Å. An RMSD < 3 Å for the C α atoms of the backbone of a template and predicted protein is considered a success [19]. With all atoms having an RMSD < 3 Å this hDAT homology model should be considered more than satisfactory.

Molecular dynamics

The validated hDAT homology model was embedded into a terminal axonal lipid bilayer membrane and surrounded by a water box using CHARMMGUI. The generated PDB and protein structure files (psf) were then utilized for molecular dynamics simulations using NAMD for minimization, equilibration, and molecular dynamics.

Ligands

The test ligands cocaine and 3,4-dichlorophenethylamine were sketched using SYBYL-X 2.1.1 and energy-minimized using Powell Method and the Tripos Force Field with Gasteiger–Hückel charges and a distance-

dependent dielectric constant of $1.0 \text{ D}/\text{\AA}$ to an energy gradient cutoff of $0.05 \text{ kcal} (\text{mol} \times \text{\AA})^{-1}$.

Docking studies

Molecular docking was conducted using the GOLD scoring function from GOLD 2020. GOLD is an optimized scoring function for the prediction of the binding orientation of small-molecules that takes into account protein-ligand hydrogen bond energy, protein-ligand van der Waals energy, ligand internal vdW energy, and ligand torsional strain energy. The test ligands cocaine and 3,4-dichlorophenethylamine were docked 100 times each into the hDAT homology model and the resultant 200 docking solutions were analyzed. The GOLD docking solutions were ranked according to their overall fitness function scores. The binding site was defined to include all atoms within 10 \AA of the carboxylic acid portion of the key amino acid residue D79 which makes an essential salt bridge interaction with the nitrogen atom of hDAT agents [20].

Compliance with ethical standards

Conflict of interest The authors declare no competing interests.

Publisher's note Springer Nature remains neutral with regard to jurisdictional claims in published maps and institutional affiliations.

References

- Aggarwal S, Mortensen OV. Overview of monoamine transporters. *Curr Protoc Pharmacol*. 2017;79:12.16.1–7. <https://doi.org/10.1002/cpph.32>.
- Yamashita A, Singh SK, Kawate T, Jin Y, Gouaux E. Crystal structure of LEUTAA, a bacterial homolog of Na^+/Cl^- -dependent neurotransmitter transporters. *Nature*. 2005;437:215–23. <https://doi.org/10.1038/nature03978>.
- Gouaux E, Penmatsa A, Wang K. X-ray structure of dopamine transporter elucidates antidepressant mechanism. *Nature*. 2013;503:85–90. <https://doi.org/10.2210/pdb4m48/pdb>.
- Wang KH, Penmatsa A, Gouaux E. Neurotransmitter and psychostimulant recognition by the dopamine transporter. *Nature*. 2015;521:322–7. <https://doi.org/10.1038/nature14431>.
- Penmatsa A, Wang KH, Gouaux E. X-ray structures of *Drosophila* dopamine transporter in complex with nisoxetine and reboxetine. *Nat Struct Mol Biol*. 2015;22:506–8. <https://doi.org/10.1038/nsmb.3029>.
- Coleman JA, Green EM, Gouaux E. X-ray structures and mechanism of the human serotonin transporter. *Nature*. 2016;532:334–9. <https://doi.org/10.1038/nature17629>.
- Coleman JA, Yang D, Zhao Z, Wen P-C, Yoshioka C, Tajkhorshid E, et al. Serotonin transporter–ibogaine complexes illuminate mechanisms of inhibition and transport. *Nature*. 2019;569:141–5. <https://doi.org/10.1038/s41586-019-1135-1>.
- Coleman JA, Navratna V, Antermite D, Yang D, Bull JA, Gouaux E. Chemical and structural investigation of the paroxetine-human serotonin transporter complex. *Elife*. 2020;9:e56427. <https://doi.org/10.1101/2020.02.26.966895>.
- Coleman JA, Gouaux E. Structural basis for recognition of diverse antidepressants by the human serotonin transporter. *Nat Struct Mol Biol*. 2018;25:170–5. <https://doi.org/10.1038/s41594-018-0026-8>.
- Huang X, Zhan C-G. How dopamine transporter interacts with dopamine: Insights from molecular modeling and simulation. *Biophys J*. 2007;93:3627–39. <https://doi.org/10.1529/biophysj.107.110924>.
- Yuan Y, Huang X, Midde NM, Quizon PM, Sun W-L, Zhu J, et al. Molecular mechanism of HIV-1 Tat interacting with human dopamine transporter. *ACS Chem Neurosci*. 2015;6:658–65. <https://doi.org/10.1021/acscchemneuro.5b00001>.
- Haddad Y, Heger Z, Adam V. Guidelines for homology modeling of dopamine, norepinephrine, and serotonin transporters. *ACS Chem Neurosci*. 2016;7:1607–13. <https://doi.org/10.1021/acscchemneuro.6b00242>.
- Ortore G, Orlandini E, Betti L, Giannaccini G, Mazzoni MR, Camodeca C, Nencetti S. Focus on human monoamine transporter selectivity. New human DAT and NET models, experimental validation, and SERT affinity exploration. *ACS Chem Neurosci*. 2020;11:3214–32. <https://doi.org/10.1021/acscchemneuro.0c00304>.
- Altschul SF, Gish W, Miller W, Myers EW, Lipman DJ. Basic local alignment search tool. *J Mol Biol*. 1990;215:403–10. [https://doi.org/10.1016/s0022-2836\(05\)80360-2](https://doi.org/10.1016/s0022-2836(05)80360-2).
- Šali A, Blundell TL. Comparative protein modelling by satisfaction of spatial restraints. *J Mol Biol*. 1993;234:779–815. <https://doi.org/10.1006/jmbi.1993.1626>.
- Melo F, Sali A. Fold assessment for comparative protein structure modeling. *Protein Sci*. 2007;16:2412–26. <https://doi.org/10.1110/ps.072895107>.
- Jo S, Kim T, Iyer VG, Im W. CHARMM-GUI: a web-based graphical user interface for CHARMM. *J Comput Chem*. 2008;29:1859–65. <https://doi.org/10.1002/jcc.20945>.
- Jones G, Willett P, Glen RC, Leach AR, Taylor R. Development and validation of a genetic algorithm for flexible docking. *J Mol Biol*. 1997;267:727–48. <https://doi.org/10.1006/jmbi.1996.0897>.
- Reva BA, Finkelstein AV, Skolnick J. What is the probability of a chance prediction of a protein structure with an RMSD of 6 \AA ? *Fold Des*. 1998;3:141–7. [https://doi.org/10.1016/s1359-0278\(98\)00019-4](https://doi.org/10.1016/s1359-0278(98)00019-4).
- Kitayama S, Shimada S, Xu H, Markham L, Donovan DM, Uhl GR. Dopamine transporter site-directed mutations differentially alter substrate transport and cocaine binding. *Proc Natl Acad Sci USA*. 1992;89:7782–5. <https://doi.org/10.1073/pnas.89.16.7782>.